

# Review

## The free energies of solid-liquid interfaces

D. R. H. JONES

*Department of Metallurgy & Materials Science, University of Cambridge, UK*

The present knowledge of crystal-melt interfacial energies is examined critically, consideration being given to the full range of metallic, inorganic and organic materials, both pure and impure. The methods currently available for measuring crystal-melt energies are discussed, and the significance of the experimental values in elucidating processes of crystal nucleation and growth is pointed out. The application of solid-liquid energy values to the measurement of other interphase boundary energies is indicated.

### 1. Introduction

The free energy,  $\gamma_{SL}$ , of the interface between a solid and its melt has a vital influence on nearly all processes involving the nucleation and growth of crystals from the molten state. For example, crystal-melt energies dictate to a large extent the temperatures at which solids nucleate (either homogeneously or heterogeneously) from their liquids [1, 2]. If the subsequent growth of the solid takes place at steps in the solid-liquid interface then the energy of the moving interface will affect the rate of transformation quite substantially [3]. Interfacial energy is often important in determining the morphology of growth [4, 5], and may also lead to solidification taking place in preferred crystallographic directions [6]. During the latter stages of solidification  $\gamma_{SL}$  enters into phenomena such as the coarsening of dendrites, the formation of gas bubbles [2], and the temperature-gradient migration of liquid inclusions [7], and even helps to determine the high-temperature stability of grain boundaries [8].

In view of the obvious importance of the liquid-to-solid transformation, it is clearly desirable to have a quantitative knowledge both of interfacial energies as such and of ways in which these energies may be modified to practical advantage. In addition, interfacial energy is one of the very few measurable quantities that enable one to gain some insight into the structural nature of the solid-liquid interface; such knowledge is not only of fundamental relevance to the physics of interfaces but, again, may lead to improved technology in the areas of crystal

growth and foundry practice.

Unfortunately, in contrast to the case of liquid-vapour energies for example, the experimental measurement of solid-liquid energies is not at all easy even for pure materials; it is even more difficult to accomplish for multi-component systems, and, consequently, lamentably little progress has been made in this latter area. As will be shown later, there are several problems to be overcome before we can use theoretical models of the solid-liquid interface to obtain reliable, calculated values of  $\gamma_{SL}$  even for simple systems. Fortunately, however, much attention has lately been aimed at devising experimental techniques designed to overcome the practical difficulties inherent in making interfacial energy measurements. Accordingly, it is pertinent first of all to review these methods and to discuss the energy values derived from them.

### 2. Experimental measurements of solid-liquid energies

Before turning to the detailed techniques of measuring  $\gamma_{SL}$  it is necessary to make some important general remarks concerning experimental values of interfacial energy. First, there is every reason to suppose that the structure of a moving solid-liquid interface, and hence its energy, depends on the interfacial velocity  $V_i$ . Thus in order to determine the value of  $\gamma_{SL}$  appropriate to any process (for example dendritic growth) we should conduct experiments using interfaces having the correct velocities, or else know  $\gamma_{SL}(V_i)$  over a sufficiently large range of velocity.

Secondly,  $\gamma_{SL}$  may depend on the dimensions of the solid-liquid system if these are less than  $0.01 \mu\text{m}$  [9-15]. Care must therefore be taken not to extrapolate  $\gamma_{SL}$  from the macroscopic to the microscopic regimes and vice versa unless the size dependence of  $\gamma_{SL}$  is known. Also important in this context is the probable influence on  $\gamma_{SL}$  of the forces emanating from surfaces or other interfaces sufficiently near to the solid-liquid interface; in certain materials this effect may be important for surfaces as far away as  $1 \mu\text{m}$  from the solid-liquid interface [16].

Thirdly, the presence of minute amounts of impurity in a solid-liquid system will allow one or more adsorbed layers to form on the solid-liquid interface, with a consequent reduction in  $\gamma_{SL}$ . Fortunately, it should still be possible to reproduce measurements of  $\gamma_{SL}$  for any material; for usually all adsorbable impurities will be present in sufficient quantity that the degree of adsorption (and thus  $\gamma_{SL}$ ) will not change appreciably with variations in impurity concentration from one specimen to another. It will, of course, be almost impossible ever to measure  $\gamma_{SL}$  for perfectly pure systems, but this is unlikely to be a practical disadvantage.

### 2.1. Direct application of the Gibbs-Thomson equation

The most powerful methods at present available for measuring  $\gamma_{SL}$  experimentally make direct use of the so-called Gibbs-Thomson equation. This thermodynamic result shows that, if all other intensive variables (such as composition, pressure and strain energy) remain constant, a solid bounded by an element of interface having principal radii of curvature  $r_1$  and  $r_2$  measured in the solid will be in equilibrium with its melt at a temperature  $T_r$  which is not equal to the phase diagram liquidus temperature  $T_m$ . The expression may be written as

$$T_m - T_r \equiv \Delta T = \gamma_{SL} \left( \frac{1}{r_1} + \frac{1}{r_2} \right) \frac{\bar{V}_{Si}}{(\bar{S}_{Li} - \bar{S}_{Si})}, \quad (1)$$

where  $\bar{V}_{Si}$ ,  $\bar{S}_{Li}$  and  $\bar{S}_{Si}$  are the partial molar values with respect to the *i*th component of the volume of the solid, the entropy of the liquid, and the entropy of the solid.  $\gamma_{SL}$  refers to the small interfacial element. In the case of a pure system having isotropic  $\gamma_{SL}$ , Equation 1 reduces to

$$T_m - T_r \equiv \Delta T = \gamma_{SL} \left( \frac{1}{r_1} + \frac{1}{r_2} \right) \frac{T_m}{L\rho_s}, \quad (2)$$

where  $L$  is the latent heat of fusion per unit mass,  $\rho_s$  is the density of the solid phase, and the equation applies to an extended (non-elemental) interface. Thus, if the appropriate physical constants are known, measurements of  $\Delta T$  for known values of  $r_1$  and  $r_2$  for a system at "equilibrium" will yield values of  $\gamma_{SL}$  directly.

There are nevertheless several practical difficulties associated with using the Gibbs-Thomson equation. First, a single crystal of solid surrounded by its melt at the equilibrium temperature is in a condition of highly unstable equilibrium; a small fluctuation will lead either to complete melting or complete solidification, and the practical attainment of "equilibrium" is thus difficult. For systems where  $r_1, r_2 \lesssim 0.1 \mu\text{m}$ ,  $\Delta T$  is sufficiently large (say 1 to 30 K) that it can be measured easily, and consequently a careful control over the intensive variables (for example impurity concentration and strain energy) is not usually important. However, surface forces (emanating from a container for instance) may affect  $\gamma_{SL}$  seriously. The reverse situation holds for  $r_1, r_2 \gtrsim 1 \mu\text{m}$ ; surface forces are usually not important, but because  $\Delta T$  is only about 0.1 K or less an exceptionally high degree of control is required over temperature and solute concentration for example.

In the next section we shall discuss the attempts, many of them very ingenious, which have been made to overcome these difficulties.

#### 2.1.1. The absolute determination of "equilibrium" temperatures

##### (a) Skapski's method

The first really successful attempts at measuring  $\gamma_{SL}$  directly from the Gibbs-Thomson equation, following on from the pioneering but somewhat equivocal work of Meissner [17], were by Skapski and his colleagues [18-20]. These authors measured  $\gamma_{SL}$  for myristic, stearic and lauric acids, and for benzene and ice-water. Using a Beckmann thermometer  $\Delta T$  was measured for systems held at temperatures of  $0.02 \pm 0.002$  to  $0.8 \pm 0.002$  K below  $T_m$ . Fig. 1a shows the elegant wedge-like geometry employed in the case of the acids for achieving "equilibrium" conditions and observing the interfacial curvatures in the transparent systems. Notice that the system is stable with respect to small fluctuations in temperature; if for example the

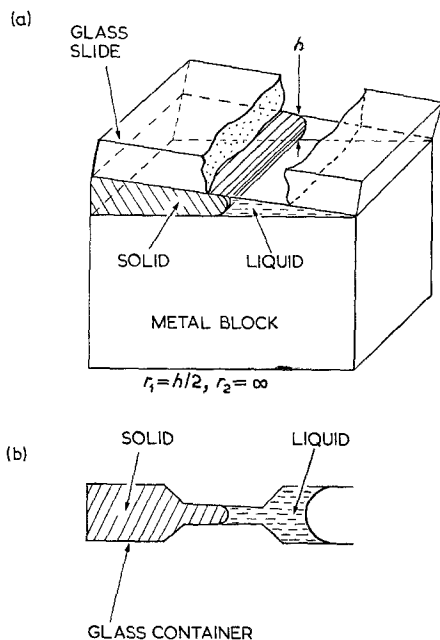


Figure 1 The arrangements devised by Skapski and his colleagues for measuring the curvatures of pure solid-liquid interfaces at various temperatures.

temperature decreases, the solid will grow so as to increase the curvature of the solid-liquid interface which, by Equation 1, restores equilibrium. A similar argument applies to small increases in temperature. The presence of the liquid-vapour meniscus causes the solid-liquid system to be at a pressure of less than one atmosphere; this leads to a related change in  $T_m$  which, fortunately in the case of the acids, is small [18]. In order to eliminate meniscus effects, Skapski devised an even more elegant arrangement employing a tapering capillary (see Fig. 1b). This apparatus also allowed  $r_1$  and  $r_2$  to be measured directly rather than, as in the earlier experiment, having to assume a cylindrical interface and having to measure separately the contact angle between the solid-liquid interface and the container. The modified arrangement was used for the work on ice-water and benzene and was also employed to check the earlier work on lauric and stearic acids.

The interfacial energy values obtained by Skapski *et al* are given in Table I. It was found, from experiments using the wedge technique, that  $\gamma_{SL}$  for stearic acid was anisotropic to about 30%. In the capillary experiments, on the other hand, the solid-liquid interfaces were reported

to be hemispherical, implying that  $\gamma_{SL}$  is isotropic for ice-water, benzene, and lauric and stearic acids (see Section 3). The apparent contradiction in the case of stearic acid probably indicates that we should not take too seriously the statement regarding the equilibrium forms of the crystals in the capillaries.

In order to achieve a reasonable accuracy it was found important, as expected, to use very pure materials and to avoid generating strain fields in the solid crystals. In the cases of benzene and ice-water (and presumably in the other capillary experiments)  $\gamma_{SL}$  was found to be independent of whether very slow melting or freezing took place at the interface. This indicates that, provided the only possible kinetic effects are due to the flow of latent heat and solute, or to the driving forces required for interfacial motion, such effects are negligible; this is because the magnitudes of these phenomena change sign as  $V_i$  changes sign. If, however,  $\gamma_{SL}$  for the "melting" interface is not the same as that for the "freezing" interface the situation is more complex as the kinetic effects may cancel out the energetic effects. Turning to the wedge experiments,  $\gamma_{SL}$  was measured only for interfaces at which slow melting took place (at a rate of *c.*  $0.5 \mu\text{m sec}^{-1}$ ). In this case the determination of  $\gamma_{SL}$  must neglect kinetic effects. Fortunately these need not be large because (a) the thermal resistivity of the system is low, and (b) the driving forces for melting are probably small – as in most materials – because of the abundance of defects at the surfaces of melting crystals.

An interesting feature of the work is the independence of  $\gamma_{SL}$  on the proximity of the container to the solid-liquid interface over a range of distances of 0.2 to 5  $\mu\text{m}$ ; this supports the earlier comments on the absence of surface-force effects for large enough systems.

In spite of the attractiveness of Skapski's method it is not suitable for handling impure systems. The technique is in principle applicable to pure metals but the associated practical problems are likely to be severe.

#### (b) Miksch's experiment

The effect of increasing the pressure acting on an ice-water system is to lower the temperature at which the two phases are in equilibrium. This principle has been used by Miksch [21] in work on the ice-water temperature standard. The experimental arrangement consisted of two ice-water

TABLE I

Substance	Nucleus-melt energies ( $\text{mJ m}^{-2}$ )	$\gamma_{\text{SL}}$ ( $\text{mJ m}^{-2}$ )			Anisotropy of $\gamma_{\text{SL}}$ (%)
		Direct values near equilibrium		Indirect values	
				near equilibrium	
Ice-water*	26.1 [54, 22] 24.2 [55, 60]	44 $\pm$ 10, C [19] 44 $\pm$ 10, GBG [36] 45 $\pm$ 15, DAC (see p. 10) 46 (see p. 5)	25 [66] (interfacial perturbation)	25 to 42 [75] 20 $\pm$ 2, DG [4]	Small [4, 23, 46]
Benzene	> 19.8 [91, 22]	44 $\pm$ 10, GBG [36] 22 $\pm$ 2, C [20]	—	—	5 [36]
White phosphorus	> 10.7 [91, 22]	12 $\pm$ 2, GBG [36]	—	0.93 $\pm$ 0.05, DG [71] 0.7, DG [73]	Negligible [34]
Naphthalene	> 27.2 [91, 22]	61 $\pm$ 11, GBG [36] 69, DMP [25]	—	—	20 [36]
Carbon tetrabromide	> 10 to > 20 [91, 22]	10 to 20, GBG [36]	—	—	0 to 6 [36]
Diphenyl	> 24 [91, 22]	50 $\pm$ 10, GBG [36]	—	—	20 [36]
Succinonitrile	—	28 $\pm$ 4, GBG [36]	—	—	} Negligible [34]
Camphene	—	6 $\pm$ 1, GBG [36]	—	—	
Ethylene dibromide	> 19.5 [91, 22]	35 $\pm$ 7, GBG [36]	—	—	0 to 15 [36]
Bismuth	> 54.4 [53]	55 to 80, DMP [12]	74 $\pm$ 3, GBE [49]	—	Small? (see p. 14)
Tin	> 59 [see 51]	62 $\pm$ 10, DMP [13]	—	—	—
Gold	> 132 [59]	270 $\pm$ 10, DMP [14]	—	—	—
Lead	> 52 to > 63 [87, 1]	40 $\pm$ 7, DMP [15]	—	—	Small (see p. 14)
Stearic acid	—	135 to 180, W [18] 180 $\pm$ 10, C [19]	—	—	30 [18]
Lauric acid	—	100 $\pm$ 15, W [19] 99 $\pm$ 5, C [19]	—	—	—
Myristic acid	—	116 $\pm$ 10, W [18]	—	—	—

\* $\gamma_{\text{SL}}$  increases approximately linearly as sodium chloride is added to the melt in the range 0 to 1 mol  $\text{kg}^{-1}$  [36]; for a melt concentration of 1 mol  $\text{kg}^{-1}$   $\gamma_{\text{SL}}$  is found to be 58  $\pm$  15  $\text{mJ m}^{-2}$  [36].

C = conical capillary, GBG = grain-boundary groove shapes, DAC = dihedral angles and contact angle, DG = dendritic growth, DMP = depression of melting point, GBE = from calculated energy of grain boundary and measured dihedral angle, W = wedge method.

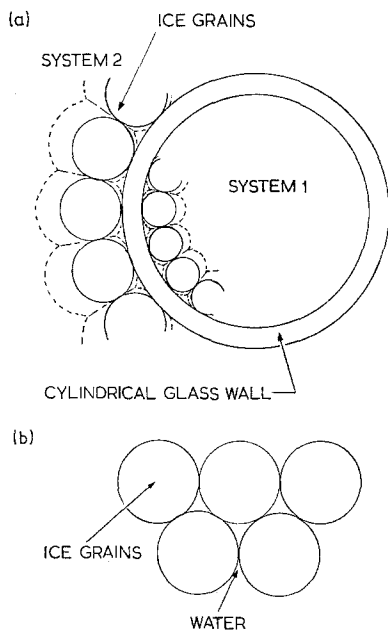


Figure 2 (a) Section taken through the ice-water systems in Miksch's experiment; (b) view of the polycrystalline ice layers in a direction perpendicular to the axis of the cylindrical glass wall. The dotted lines indicate the positions that would be adopted by the ice-water interfaces were the system temperatures to decrease.

systems (Fig. 2a) at a common temperature but subjected to different pressures. In each system the ice was in the form of a polycrystalline layer one crystal thick deposited on glass. During the experiments it was found that, in order to maintain "equilibrium" in each system, a pressure difference (equivalent to a temperature difference of  $2.9 \times 10^{-5}$  K) was required between the systems; this was attributed to the systems having different grain sizes (*c.* 2 and 3 mm respectively) and hence different interfacial curvatures.

Although Miksch did not measure the interfacial radii these have been estimated from the grain sizes by the present author [22]. This derivation used the information that, for ice-water, (a)  $\gamma_{SL}$  is isotropic (see Table I), (b) the dihedral angle at the intersection of the solid-liquid interface with a high-angle grain boundary is about  $30^\circ$  when measured in the liquid [23, 24], (c) the angle of contact of the solid-liquid interface with glass is  $0^\circ$  measured in the liquid [19]. The structure of the ice layers consistent with these data is shown in Fig. 2b. A resulting figure for  $\gamma_{SL}$  of about  $46 \text{ m J m}^{-2}$  was obtained [22] from the analysis. This value is in excellent

agreement with the other direct figures for ice-water (Table I) although the agreement may be somewhat fortuitous in view of the uncertainty in the measured grain sizes. Nevertheless, the present result is quoted because of a unique feature of the method – the extremely low interfacial velocities encountered (nominally as small as 0.01 molecular diameters a second for both melting and freezing). It is unlikely that a much closer approach to equilibrium can ever be attained in practice, and it would be of considerable interest to repeat the experiments making more careful measurements of grain size.

It should be noted that the ice layers in system 2 (but not in system 1) are somewhat unstable; if the temperature decreases, for example, growth will occur so as to cause a further departure from equilibrium (Fig. 2a). The exceptionally low  $V_i$  were achieved by having very steady temperatures (provided by an ice-water bath) and by adjusting the pressures over many days. It thus seems unlikely that this technique can be applied to substances other than very pure water.

### (c) The melting points of small crystals

If a small, isolated crystal is heated, melting should begin at the crystal-vapour interface and the crystal should become surrounded by a thin shell of liquid provided the crystal size is initially  $\lesssim 1 \text{ nm}$  [12]. At first the liquid skin will be too thin for the liquid to be thought of as having the properties of the bulk phase; but when the skin has achieved a critical thickness,  $t$ , the Gibbs-Thomson equation may be used to derive a relationship between  $r_1$ ,  $r_2$  and  $T_r$  under equilibrium conditions. In this connection  $T_m$  must be corrected to allow for the pressure exerted by the liquid meniscus, and the solid must be large enough to have its bulk properties. If there is no energy barrier to the formation of a liquid shell of critical thickness at  $T_r$ , a final equation may readily be obtained to describe the melting temperature of a pure spherical crystal in terms of its initial radius  $R$ , with the two adjustable parameters  $\gamma_{SL}$  (assumed isotropic) and  $t$ . The expression may be written as [13]

$$T_m - T_r = \frac{2T_m}{L} \left\{ \frac{\gamma_{SL}}{\rho_S (R - t)} + \frac{\gamma_{LV}}{R} \left( \frac{1}{\rho_S} - \frac{1}{\rho_L} \right) \right\}, \quad (3)$$

where  $\gamma_{LV}$  is the liquid-vapour surface tension, and  $\rho_L$  is the density of the liquid. If, on the other hand, there is an energy barrier to the formation of the liquid shell at  $T_F$ , Equation 3 must be replaced by a more complex relation involving an additional adjustable parameter  $\Delta\gamma$  (given by  $\gamma_{SV} - \gamma_{SL} - \gamma_{LV}$ , where  $\gamma_{SV}$  is the solid-vapour surface tension) [12]. The appropriate equation characterizing a set of experimental  $\Delta T(R)$  data for a suitable material is that which gives the best fit between theory and experiment. Clearly, by fitting the appropriate equation to the  $\Delta T(R)$  data either  $\gamma_{SL}$  and  $t$ , or  $\gamma_{SL}$ ,  $t$  and  $\Delta\gamma$  may be found.

Experimental studies of the melting-point depressions of small crystals have been made by the group at Imperial College for tin [13], bismuth [12], gold [14] and lead [15], and by Kanig [25] for naphthalene. In the experiments on the metals and bismuth small crystals (usually 10 to 100 nm in size) were formed on carbon [12-15] or silicon monoxide [12, 13, 15] substrates by vapour deposition *in vacuo*. The onset of melting was detected either by electron diffraction (for tin, bismuth and lead) or by measuring changes in the rate of evaporation (for gold). Crystal sizes were measured by electron microscopy. Since the melting point depressions encountered were usually between 10 and 200 K they were readily measurable by direct thermometry.

It was found that Equation 3 was appropriate to the  $\Delta T(R)$  data for the metals, but not for bismuth. In the former instance it was possible to determine quite accurate values for  $\gamma_{SL}$  (Table I); but in the case of bismuth it was found that the alternative equation gave the best fit and, not surprisingly with three adjustable parameters, the accuracy achieved in  $\gamma_{SL}$  was somewhat poorer (Table I).

In the work on tin, bismuth and lead no contamination of the material could be detected from the nature of the diffraction patterns, but this need not mean that the systems were more than moderately clean. In the studies on lead and bismuth, the introduction of hydrogen was found to have no effect, indicating little oxidation. For tin, bismuth and lead no difference in behaviour was found with the two substrate materials used; but this does not constitute proof that the presence of a substrate does not lead to melting by a mechanism other than uniform surface melting. The assumption of the latter mode of melting in the theory seems to be the

primary source of uncertainty in the method. It thus seems important either to make a theoretical investigation of possible modes of melting on a substrate, or to use substrates of quite different characters; the latter might also help to indicate whether or not forces emanating from the substrate affect  $\gamma_{SL}$ . The apparent independence of energy on particle radius does not necessarily show that  $\gamma_{SL}$  is independent of interfacial curvature because size effects due to curvature and surface forces may act in opposition.

It is important in work of this type to conduct an independent verification of the isotropy of  $\gamma_{SL}$ . Among the materials studied above this has been achieved for lead and possibly bismuth (Table I). In the case of naphthalene, however,  $\gamma_{SL}$  has a 20% anisotropy (Table I); this may explain why Kanig's value is a little higher than a somewhat more direct figure for this substance (Table I).

A related method of measuring  $\gamma_{SL}$  has been indicated by Kubelka and Prokscha [26]. These authors measured the depressions of the melting points of ice, and solid benzene and ethylene dibromide, adsorbed in porous media such as silica gel. The geometry assumed for the equilibrium configuration of the adsorbed material when partly molten is shown in Fig. 3, the pores containing the adsorbate being taken to be cylindrical. In this case  $\Delta T$  and  $R$  may be related by Equation 3 provided that  $t$  is set equal to zero, and that the + sign is changed to a - sign to allow for the change in sign of the pressure exerted by the liquid meniscus [26].

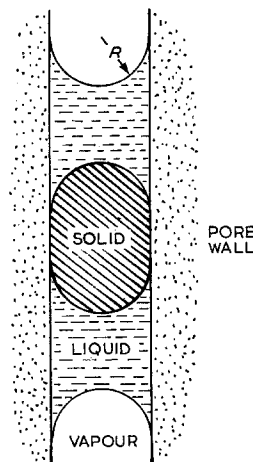


Figure 3 The assumed configuration, at "equilibrium", of a pure solid-liquid system adsorbed in a pore.

During the experiments the melting of the adsorbed solid was detected by observing changes in the vapour pressure of the adsorbate with temperature. The pore radii were found indirectly by measuring the vapour pressure of the adsorbed liquid and applying the Kelvin relation. Typical values of  $R$  and  $\Delta T$  were 10 nm and 10 K. Similar experiments were subsequently carried out by Puri and colleagues [27, 28]. Only in the earlier work [26] was  $\gamma_{SL}$  evaluated from the experimental data. The present author [22] has recalculated the value for benzene from these data and has also analysed the results of the later work. However, the values obtained are not quoted here in view of the following reasons for thinking the technique to be unsound. (a) The values of  $\gamma_{SL}$  for a given material are sometimes inconsistent from one experiment to another. (b) The values of  $R$  may be in error; it has been reported that liquids in capillaries closed at one end have abnormally low vapour pressures [29-31]. (c) The effect of surface forces on material adsorbed in a capillary is probably very large [32].

### 2.1.2. The relative determination of "equilibrium" temperatures

#### (a) The shapes of grain-boundary grooves in a temperature gradient

Probably the most attractive method of measuring  $\gamma_{SL}$  directly for macroscopic systems involves observing the "equilibrium" shapes of grooves formed by the intersection of planar grain boundaries with an otherwise planar solid-liquid interface in a system subjected to a temperature gradient. The technique is especially convenient because it does not require a high degree of temperature control and measurement, and because it allows  $\gamma_{SL}$  to be determined not only for pure materials, but also for multi-component systems.

The geometry required of the grain-boundary groove is shown in Fig. 4. At a large distance away from the grain boundary the solid-liquid interface is planar and consequently is at a temperature  $T_m$ . On going towards the root of the groove the curvature of the interface in the  $x$ - $y$  plane increases so as to balance the decreasing interfacial temperature according to the Gibbs-Thomson equation. The equilibrium shape of the groove has been calculated theoretically for the case of isotropic  $\gamma_{SL}$  [6, 33] in terms of  $\gamma_{SL}$ , the thermal conductivities of liquid and solid ( $K_S$  and  $K_L$ ),  $(S_{Li} - S_{Si})/\bar{V}_{Si}$ , and the

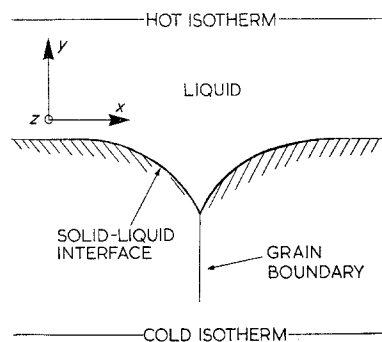


Figure 4 Schematic illustration of a grain-boundary groove formed at a solid-liquid interface in a temperature gradient. The groove shape is independent of the  $z$  co-ordinate.

temperature gradient in either liquid or solid; thus if groove shapes can be measured in known temperature gradients,  $\gamma_{SL}$  can be found directly. The method holds for impure systems [34, 35], because if  $V_i$  is small enough the solute concentration in the melt is constant and independent of  $T_r$  (as required by Equations 1 and 2).

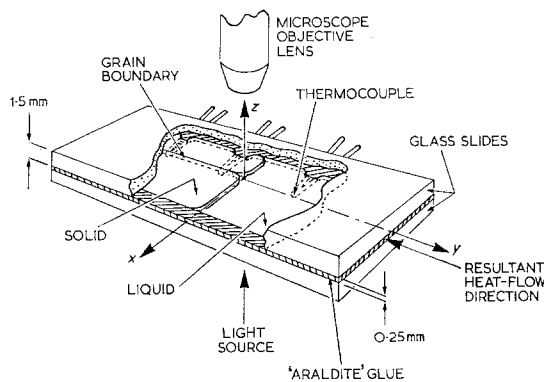


Figure 5 Experimental arrangement employed by the author for observing grain-boundary grooves in transparent materials.

In the first really successful application of the method  $\gamma_{SL}$  was measured for a range of transparent organic materials, and for white phosphorus, ice-water, and ice-water-sodium chloride systems [36]. The experimental arrangement employed in the work is shown in Fig. 5. The specimen systems were held in glass-walled cells and the required temperature gradient was generated by mounting the cells in a suitable

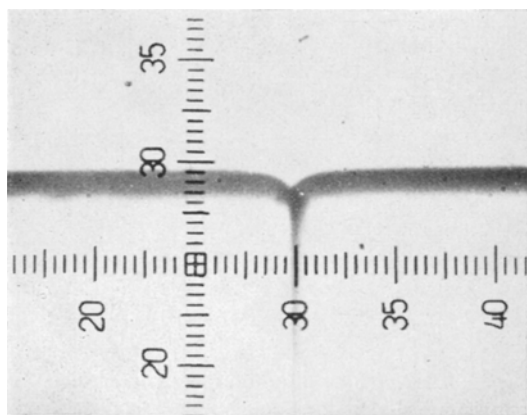


Figure 6 A typical micrograph of a grain-boundary groove in a transparent material (in this case camphene).  $\times 318$ .

heating stage. The stage was attached to an optical microscope, allowing the cross-section of the "equilibrated" grain-boundary grooves to be observed in transmitted light [22, 34, 35, 37]. A typical micrograph of a grain-boundary groove is shown in Fig. 6.

The interfacial energies obtained from the latter studies are given in Table I. In all materials other than benzene these energies agree very well with the figures derived by other direct methods. The discrepancy in the case of benzene is puzzling, however, particularly as the author's value is exactly twice that derived using the capillary method. In most cases  $\gamma_{SL}$  was measured for grooves that were "stationary" and also for grooves at which both melting and freezing took place (at rates of up to about  $0.5 \mu\text{m sec}^{-1}$ ); but no dependence of  $\gamma_{SL}$  on  $V_i$  was observed.  $\gamma_{SL}$  was found to depend linearly on salt concentration in the ice-water-sodium chloride system (Table I). On the other hand, although the concentration of impurities varied from 0 to 2 mol % in diphenyl, carbon tetrabromide and benzene, no variation of  $\gamma_{SL}$  with impurity content was detected in these chemicals. The assumption of isotropic  $\gamma_{SL}$  was verified (by conducting subsidiary experiments) for most of the materials studied (Table I).

As derived, the groove shape theory applies to the experimental geometry shown in Fig. 7, where the flow of heat through the specimen is entirely uniaxial except near the groove. In the work on the transparent materials the dimensions and thermal conductivities of both container and

specimen were comparable and it was necessary to modify the theory [36] to take into account the non-axial heat flow pattern.

The only other material for which  $\gamma_{SL}$  has been determined by the groove-shape method is lead [33, 38]. The experimental arrangement employed [38] is shown in Fig. 7. In order to observe the groove shapes a small amount of antimony was rejected into the molten lead ahead of the solid-liquid interface. After allowing time for equilibration the specimen was quenched and sectioned. The antimony-rich area was detected by etching, and the shapes of the grooves were taken to be those of the lines dividing the pure lead from the impure lead.

The value obtained for the solid-liquid energy of lead is not quoted here, however, because the treatment of the results by Nash and Glicksman [33] (who only studied one groove shape) was only intended as a demonstration of their method of analysis; it was not meant to provide a valid figure for  $\gamma_{SL}$ . This restriction apart, it is somewhat unlikely that the shapes observed in the quenched specimens [38] represent the true equilibrium shapes of the grooves. In view of the large sizes of the specimens it would have been likely that, during the quench, the solid-liquid interface would have moved some distance before fresh solid nucleated and grew ahead of the interface; and during this process the shape of the groove would have been distorted significantly by the quickly changing heat-flow pattern and by the rapid rejection of solute. It might have been possible to gain an idea of the effect by comparing groove shapes obtained from the specimen surface with those obtained from the centre of the specimen; but this does not seem to have been attempted. In any event, it is highly desirable to make direct observations of grooves in order that (a) the approach to equilibrium of the groove shape can be followed, and (b) the interfacial energies may be measured as a function of interfacial velocity.

In conclusion, it should prove relatively easy to apply the author's thin specimen technique to the study of metallic systems. Groove shapes in the latter may, for example, be observed in principle by using X-ray, ultra-violet or infra-red methods. Although these techniques have not yet been applied to studying equilibrated grain-boundary grooves, their suitability for such studies is apparent from other work on solid-liquid systems [39-41]. Thus the application of the method to the direct measurement of inter-



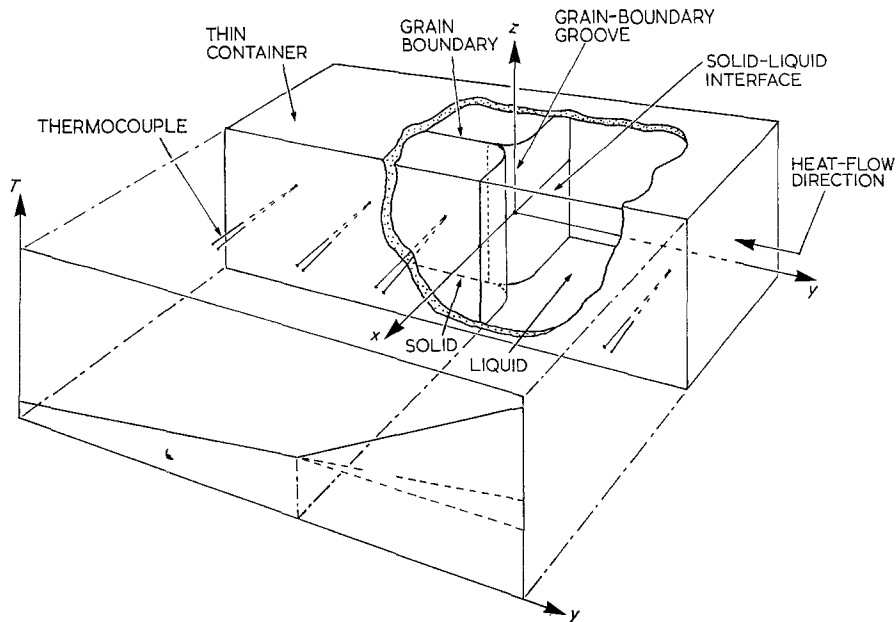


Figure 7 Experimental arrangement employed for generating grain-boundary grooves in lead.

facial energies in metals and alloys should prove very fruitful.

(b) *Liquid inclusions stationary in a temperature gradient*

We shall now indicate a new method of measuring  $\gamma_{SL}$  that has many of the advantages of the groove-shape technique, but which may give more satisfactory results at extremely high levels of solute concentration; in fact the technique can be applied only to impure systems. At a sufficiently high temperature an impure solid will usually contain a large number of small droplets (*c.* 1 to 100  $\mu\text{m}$  in size) of impure, segregated liquid. If a temperature gradient  $G$  is imposed on the solid these droplets will migrate up the temperature gradient by a combination of dissolution and solidification at the high- and low-temperature interfaces respectively, and solute flow across the droplet [7]. It is often possible, however, to observe droplets that have become immobilized even though subjected to a temperature gradient. This may be caused by the interaction of the droplet with a grain boundary perpendicular to the temperature gradient [42] as shown in Fig. 8a; alternatively, in systems where dissolution requires crystal defects (such as screw dislocations) droplets may be immobilized as a consequence of the lack of a suitable defect at the high-temperature interface [43, 44] (Fig. 8b).

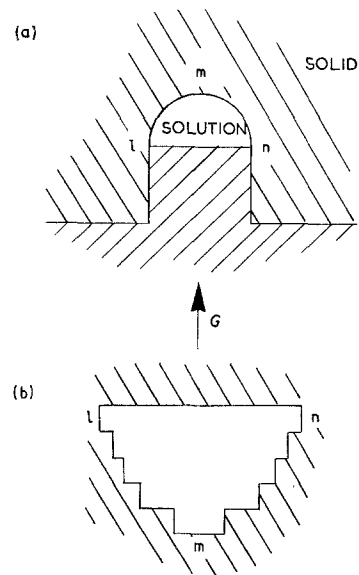


Figure 8 Schematic illustrations of impure liquid droplets immobilized in a solid subjected to a temperature gradient  $G$ .

When the solid-liquid interfaces not affected by the immobilization processes (labelled l-m-n in the figures) have reached equilibrium their shapes may again be described by the Gibbs-Thomson equation; this is because the solute concentration in the stationary droplet must be quite uniform. Thus appropriate figures may, in

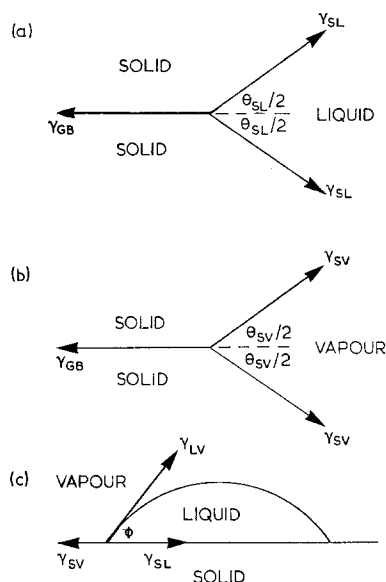


Figure 9 Schematic arrangements at three-phase junctions.

principle, be obtained for  $\gamma_{SL}$ . Clearly the analysis of droplet shapes will be most convenient for systems having  $K_S = K_L$  (allowing the thermal distribution at the interface to be calculated easily) and having simple droplet geometries.

## 2.2. Equilibria at three-phase junctions

When a grain boundary intersects a solid-liquid interface (Fig. 9a) the condition for equilibrium at the three-phase junction is

$$\gamma_{GB} = 2\gamma_{SL} \cos(\theta_{SL}/2), \quad (4a)$$

where  $\gamma_{GB}$  is the grain-boundary energy. Similarly, for the solid-vapour case (Fig. 9b),

$$\gamma_{GB} = 2\gamma_{SV} \cos(\theta_{SV}/2). \quad (4b)$$

For "equilibrium" at the edge of a liquid drop that has recently been placed on a soft, solid surface, as shown in Fig. 9c, we have

$$\gamma_{SV} = \gamma_{SL} + \gamma_{LV} \cos \phi, \quad (4c)$$

where  $\phi$  is the contact angle. The above equations all assume that the interphase energies are isotropic.

If we consider only high-angle grain boundaries then, for any suitable, pure material, we may combine Equations 4 to find  $\gamma_{SL}$  provided  $\theta_{SL}$ ,  $\theta_{SV}$ ,  $\phi$  and  $\gamma_{LV}$  are known. This principle has been used by Ketcham and Hobbs to measure  $\gamma_{SL}$  for ice-water [23]. A value of  $33 \pm 3$  mJ

$m^{-2}$  was determined, it being concluded that the anisotropy of the interphase energies was small. The latter observation is in agreement with the results of other work on this system (Table I).

The value of the ice-water energy measured by the Ketcham and Hobbs technique is, however, particularly sensitive to the measured value of  $\theta_{SV}$ . Suzuki and Kuroiwa [45] have recently shown that the real values of this angle are probably  $6^\circ \pm 3^\circ$  less than those measured via a replica technique by Ketcham and Hobbs because the replicating solution used by the latter workers attacks ice. An appropriate correction to the angles measured by Ketcham and Hobbs yields a value for  $\gamma_{SL}$  of  $45 \pm 15$  mJ  $m^{-2}$ , in excellent agreement with all other direct values measured for the ice-water interface at equilibrium (Table I). The value for the contact angle of  $1^\circ$  measured by Ketcham and Hobbs has recently been questioned by Knight [46] who estimated that this quantity might be as large as  $10^\circ$ ; but, fortunately,  $\gamma_{SL}$  is insensitive to variations in contact angle of between  $0^\circ$  and  $20^\circ$ .

The technique does not appear to have been applied to any other pure materials, but has been used for highly dissimilar phases such as solid copper and liquid lead. However, in such cases the method is not necessarily valid. When measuring  $\theta_{SV}$  both the grain boundary and solid surface are pure; but when determining  $\theta_{SL}$  the grain boundary is often highly contaminated by the liquid phase, and  $\gamma_{GB}$  cannot always be eliminated from the equations as is necessary. In the sessile drop experiment for measuring  $\phi$  the drop material must often contaminate the solid surface, and thus neither can  $\gamma_{SV}$  necessarily be assumed constant from one equation to another. In view of these obvious pitfalls we shall not refer again to any experimental studies involving the use of sessile-drop techniques in multi-component systems.

A somewhat related, but less direct, method of measuring interfacial energy has been described by Glicksman and his co-workers [47-49]. In this work measurements were made of the dihedral angles formed by the intersection of low-angle, symmetrical-tilt grain boundaries with a solid-liquid interface in pure bismuth. The specimens were present as thin layers, the experimental and thermal configurations being closely analogous to those shown in Fig. 5; but the groove shapes were observed in the electron microscope and the temperature gradient desirable for stability of the groove was generated by

electron-beam heating of the liquid. The misorientations across the grain boundaries were measured *in situ* by diffraction techniques, and the energies of the boundaries were determined from the Read-Shockley formula together with the known elastic constants for bismuth.  $\gamma_{SL}$  was found from the calculated values of  $\gamma_{GB}$  by balancing surface tensions at each groove (Equation 4a) and was shown to be  $74 \pm 3$  mJ m<sup>-2</sup>. This value agrees favourably with that obtained by Coombes [12] from melting point data (see Table I). It should be noted that the Read-Shockley formula is not completely valid in the above experimental situation [47]; unfortunately, the error so resulting in the present value of  $\gamma_{SL}$  does not yet appear to be calculable [47]. In addition, the present calculation of  $\gamma_{GB}$ , and hence that of  $\gamma_{SL}$ , can only be made for a clean system; the value of  $\gamma_{SL}$  computed by this method is therefore not necessarily applicable to a real (contaminated) system. Another possible error may stem from the fact that the dihedral angles were measured for solid-liquid interfaces less than about 0.05  $\mu$ m apart. The measured angle may have been affected by surface forces emanating from the interfaces; and this could be important in view of the large values of  $\theta_{SL}$ , and consequent sensitivity of the measured interfacial energy to the observed geometry. In general there may be difficulties in applying this technique to materials other than bismuth; certainly the method would be most awkward to use in the case of impure systems because of the difficulty of calculating the grain-boundary energy with sufficient accuracy.

Before leaving the subject of surface-tension equilibria, it is worth pointing out the usefulness of these phenomena in determining other interphase energies from a knowledge of  $\gamma_{SL}$ . Clearly, if  $\gamma_{SL}$  is known, the measurement of  $\theta_{SL}$  in any material, pure or impure, will yield experimental values of  $\gamma_{GB}$ . As an example for a pure system, we may compute a revised value of  $84 \pm 20$  mJ m<sup>-2</sup> for the energy of a high-angle grain boundary in ice from the modified data mentioned above. In the case of impure materials,  $\theta_{SL}$  can be measured very easily [8], and it should prove possible to determine  $\gamma_{GB}$  for such systems by measuring  $\gamma_{SL}$  via the groove-shape technique. Similar methods should also allow the determination of solid-state interphase energies in both eutectic and non-eutectic systems. With regard to pure materials,

the sessile drop technique permits the determination of  $\gamma_{SV}$  from  $\gamma_{SL}$  and vice versa. By way of example we may derive a revised value for the ice-vapour energy of  $120 \pm 10$  mJ m<sup>-2</sup> from the relevant data. Finally, it is noteworthy that accurate values have recently been determined for solid-vapour energies (as in the work at Imperial College on the vapour pressures of small crystals) and thus the sessile drop method should afford a useful means of corroborating experimental figures for  $\gamma_{SV}$  and  $\gamma_{SL}$  in the case of pure materials.

### 2.3. Crystal nucleation

Until recently almost all experimental values of  $\gamma_{SL}$  were obtained from experiments involving the supposed homogeneous nucleation of solid from an undercooled melt. The results were analysed according to the theory of homogeneous nucleation developed by Turnbull and Fisher [50], and nucleus-melt energies were obtained for a wide range of metals, metalloids, and organic and inorganic substances (see the reviews by Holloman and Turnbull [51] and Jackson [52] for example).

There are, nonetheless, several problems associated with this technique. First, only in mercury [53] and ice-water [see, for example, refs. 54 and 55] has the assumption of homogeneous nucleation been verified experimentally. In the absence of such verification the values of  $\gamma_{SL}$  obtained can only be taken to be minima. Indeed, in several cases [1, 51, 56, 57], the undercoolings required to cause nucleation have been found to be substantially larger than those reported by earlier workers [58, 59], indicating heterogeneous nucleation in the earlier studies.

Secondly, a difficulty in interpreting the results arises from the fact that the free energy of formation of the solid nucleus may vary in a complex manner with temperature. A correct expression for deriving the energy of formation has recently been formulated by the author [22, 60], rendering the theory of nucleation thermodynamically self-consistent. Using this expression the values of  $\gamma_{SL}$  obtained from the simple theory [50] need to be decreased by up to 15% for non-metals, but by only *c.* 1% for most metals.

Thirdly, it has been suggested [1] that a quantum-mechanical, correction term should be included in the nucleation rate equation. In the case of metals, organic compounds, and ice-water this term implies that  $\gamma_{SL}$  values derived

from simple theory should be increased by 0 to 7% to arrive at the correct values [1, 22]; but it does not seem possible to specify the extent of the correction more closely than this.

A further difficulty arises from the fact that, in nucleation experiments,  $\gamma_{SL}$  is determined at temperatures as much as 200 K below  $T_m$ . Thus nucleus-melt energies cannot be equated to macroscopic energies without information on the temperature coefficient of interfacial energy (at the present unknown).

Finally, there are the well-known uncertainties inherent in applying macroscopic thermodynamics to systems as small as the solid nucleus (typically *c.* 1 nm in size). In this context, if the solid-liquid interface is at all diffuse, values of  $\gamma_{SL}$  measured in nucleation may be significantly less than those measured for macroscopic interfaces [61].

Values of nucleus-melt energies, corrected as indicated above, are listed in Table I for those substances for which other values of  $\gamma_{SL}$  are known. As is clear from the table, the direct figures for  $\gamma_{SL}$  for systems at equilibrium are almost invariably much greater than the corrected nucleus-melt energies; but this need not necessarily support the diffuse interface hypothesis. It should be mentioned that the tabulated nucleus-melt energies have been calculated assuming the solid nucleus to be roughly spherical. With regard to ice-water, some workers have assumed that the nucleus is a hexagonal prism [see, for example, 62-64]; but this assumption seems quite ill-founded simply because the energies associated with the edges of such a body would almost certainly be far too high relative to the face energies to allow it to exist. Because of this and other differences of interpretation of the data for ice-water the values of the nucleus-melt energy in the literature are not always in mutual agreement (see the discussion by the present author [22]). The values tabulated for the nucleus-melt energy of ice-water are the most accurate at present available.

In conclusion, although the nucleation technique is not suitable for measuring macroscopic solid-liquid energies, it may well provide information on the structures of crystal-melt interfaces in pure materials. In contrast, the interpretation of data on impure systems [65] is likely to be too complex to be of immediate value.

## 2.4. Crystal growth

### 2.4.1. Shape instability of a solid-liquid interface during solidification

As is well known, in many materials the solid-liquid interface adopts a smooth, non-faceted form (free of small hummocks) during slow growth from the melt. This mode of solidification is usually referred to as "planar" growth. If, however, the velocity of growth is increased sufficiently this morphology becomes unstable and small protrusions form at the solid-liquid interface. The probability of such protrusions forming is governed partly by  $\gamma_{SL}$  since, clearly, their existence results in a higher interfacial area and a consequent increase in the energy of the system. If suitable measurements are made of the formation of interfacial protrusions, the data may be analysed according to the Mullins-Sekerka theory of interfacial instability, yielding  $\gamma_{SL}$ .

This principle has been employed by Hardy and Coriell to measure  $\gamma_{SL}$  for ice-water [4, 66, 68], and for the interfaces between ice and various dilute aqueous solutions [66, 67]. Direct observations were made of interfacial morphology during the slow radial growth (at *c.* 0.1  $\mu\text{m sec}^{-1}$ ) of ice cylinders having axes parallel to the *c*-axis of ice. After successive refinements of the technique (during which the resulting value of  $\gamma_{SL}$  rose step-by-step from an initial value of 16  $\text{mJ m}^{-2}$ ), a final figure of 25  $\text{mJ m}^{-2}$  was obtained for pure ice-water. In addition, quantitative proof was found that the anisotropy of  $\gamma_{SL}$  is small [4]. With the slightly impure systems  $\gamma_{SL}$  was normally about 1 or 2  $\text{mJ m}^{-2}$  different from the value for pure ice-water; but measurements were not made over sufficiently large ranges of solute concentration for the concentration dependences of  $\gamma_{SL}$  to be measured accurately. It is surprising to see that the value obtained with the technique is almost half that derived by the direct methods (see Table I) even though  $V_1$  is small. This may well indicate a basic problem in the application of the Mullins-Sekerka theory to experiments of the present type [69].

In conclusion the method can, in principle, be extended to opaque systems as in these cases the propagation of interfacial instabilities may be observed by using ultra-sonic techniques. However, the latter may not be well suited to quantitative work because of the associated generation of energy at the solid-liquid interface.

#### 2.4.2. Dendritic growth

It has long been known that many materials solidify from their melts in the form of branched needle-like crystals, or dendrites. However, only recently has a rigorous quantitative description been made of this complex process [see, for example, 5]. This treatment, due to Temkin [70], applies to the special case of an *isolated* unbranched dendrite (having the shape of a semi-infinite paraboloid of revolution and having linear interfacial kinetics) growing from a pure melt at an otherwise uniform temperature  $T_B$ . When both the velocity of the dendrite tip,  $V_i$  (tip), and  $T_B$  have been measured, and physical constants such as  $K_S$ ,  $K_L$ , and  $L$  have been found, there remain two unknown quantities in the theory; these are the kinetic constant of the solidification reaction,  $\mu$ , and  $\gamma_{SL}$ . If enough pairs of values of  $V_i$  (tip) and  $T_B$  can be obtained, and  $V_i$  is sufficiently low, both  $\mu$  and  $\gamma_{SL}$  can be obtained by analysing the data using the computer programme available from Kotler and Tarshis.

By applying their programme to the results obtained by Lindenmeyer, Kotler and Tarshis found  $\gamma_{SL}$  to be  $20 \pm 2 \text{ mJ m}^{-2}$  for ice-water interfaces moving at between 1 and 20 mm sec<sup>-1</sup> [5]. That this figure is less than half the value measured directly under near-equilibrium conditions may well indicate a pronounced dependence of  $\gamma_{SL}$  on  $V_i$  for aqueous systems. Kotler and Tarshis [5] also analysed data for pure tin but, unfortunately, these results were too scattered to allow an absolute measurement of  $\gamma_{SL}$  to be made.

In another paper [71] Kotler and Tarshis analysed data on assumed dendritic growth in white phosphorus obtained by Glicksman and Schaefer [72]. They obtained the astonishingly low figure for  $\gamma_{SL}$  of  $0.93 \pm 0.05 \text{ mJ m}^{-2}$  (see Table I); a similar value of 0.7 was obtained by Trivedi [73], using a more rigorous analysis. These low figures may reflect the effect on the interfacial structure of the unusually high transformation velocities encountered (100 to 2000 mm sec<sup>-1</sup>); they may also indicate that the theory is not applicable [73] partly because of the close proximity of neighbouring dendrites. However, it is highly likely that white phosphorus does not solidify dendritically in any case. The only evidence for this mode of growth is indirect, based on light scattering experiments [72]; the observed scattering behaviour was attributed to interdendritic liquid, but could,

equally, have been caused by liquid trapped between faceted needle crystals of the form observed directly by the author (unpublished work) at lower velocities.

In conclusion it would be most interesting to apply the dendritic growth technique to other pure materials, especially metals, partly in order to investigate the effect of rapid growth on  $\gamma_{SL}$ . It should also prove possible to examine impure systems, as a rigorous analysis (apparently unpublished) exists [74] for dendritic growth from alloyed melts.

A somewhat related method, employed by Fernandez and Barduhn [75], involved the slow growth (at 10  $\mu\text{m sec}^{-1}$  to 1 mm sec<sup>-1</sup>) of pure ice platelets into rapidly moving, undercooled water of temperature  $T_B$ . The interfacial temperature  $T_i$  was calculated from the  $V_i$  and  $T_B$  data by applying heat-transfer theory.  $T_i$  was then related to the known curvature of the tip of the growing crystal by Equation 2, yielding values of the ice-water energy of between 25 and 42 mJ m<sup>-2</sup>. It is interesting that these figures, referring as they do to intermediate values of  $V_i$ , lie midway between the equilibrium value and that obtained from the dendritic growth data. This, again, supports the idea of a velocity dependent interfacial structure in the ice-water system.

#### 2.4.3. The shape relaxation of liquid inclusions in isothermal solids

Under the driving force of capillarity the shape of an extended droplet of segregated liquid in a solid will change to decrease its interfacial energy. The rate of relaxation will be controlled by the transfer of solvent through the liquid and by the kinetics of the solid-liquid interface. Using this principle Cline and Anthony [76] derived a rough value of about 12 mJ m<sup>-2</sup> for the energy of the interface between KCl and an aqueous KCl solution at room temperature. Because of the sluggish interfacial kinetics in the chosen system, the derivation of  $\gamma_{SL}$  required a knowledge of the form of the kinetic law; this was determined in a subsidiary experiment involving the migration of a brine inclusion through a KCl crystal in a temperature gradient. It should be less tedious, however, to measure  $\gamma_{SL}$  for metallic systems by this method because the appropriate interfacial kinetics may well be negligible. In this connection the three-dimensional shapes of inclusions in quenched specimens may be observed radiographically [77], making it possible to observe

the relaxation of a single droplet by repeatedly quenching and annealing a thin specimen.

### 3. Anisotropy of interfacial energy

The variation in  $\gamma_{SL}$  with the crystallographic orientation of the solid-liquid interface may, in principle, be determined using several of the above experimental techniques. For example, when using the groove-shape method (Section 2.1.2.a), it can be arranged to expose preferentially a certain crystallographic plane at the surface of a given groove; the value of  $\gamma_{SL}$  relating to the groove and hence to the given crystallographic plane can then be found, and the procedure repeated to obtain  $\gamma_{SL}$  as a function of crystallographic orientation. However, such a technique, involving repeated absolute measurements of  $\gamma_{SL}$ , is laborious; and a simpler method exists for making *relative* determinations of  $\gamma_{SL}$  in a given system. This method arises from the fact that the Wulff construction allows anisotropy to be determined (within limits) from the equilibrium shapes of crystals in an isothermal melt (or conversely the equilibrium shapes of necessarily impure liquid droplets in isothermal solids). The application of the Wulff construction in this context has been discussed in detail by Miller and Chadwick [78] and will not be repeated here. It will be sufficient to remark that spherical equilibrium forms indicate isotropic  $\gamma_{SL}$ , and that non-spherical forms indicate anisotropic  $\gamma_{SL}$ .

Using this method, Miller and his colleagues [78-80] determined anisotropies from the shapes of highly impure metallic liquid droplets entrained in solid zinc, cadmium, magnesium, bismuth, antimony, aluminium, silver, copper and lead. This work has been reviewed by Chadwick [81] and Basterfield, Miller and Weatherly [82] and will be discussed only in relation to materials for which  $\gamma_{SL}$  has been measured absolutely (Table I). In this context the lead-alloy interface was found to have an anisotropy of  $\gamma_{SL}$  of less than 20% [80] even for high alloy contents. Since, in general, anisotropy has been shown to decrease with decreasing solute content [78, 81], the anisotropy of  $\gamma_{SL}$  for pure lead should be much smaller than 20% (Table I). In the case of bismuth, droplet shapes were observed at two temperatures [78] such that we find a small extrapolated anisotropy at the melting point (Table I) for planes containing "cube" directions.

The author has observed the equilibrium

shapes of liquid droplets (at *c.* 10 K below the melting point of the surrounding solid) in solid white phosphorus, and in a number of solid organic substances [22, 34, 36]. The resulting anisotropies are – except in the cases of naphthalene and diphenyl – either small or negligible (see Table I). In view of the high equilibrium temperatures, these anisotropies almost certainly relate to the pure materials – in contrast to the case for the metallic systems studied above.

It should be pointed out that anisotropies derived from droplet shapes may often be maximum values. This arises from the fact that the reactions at the solid-liquid interface sometimes prevent [76] the droplet achieving its equilibrium form. Such effects are likely to be more serious in the case of highly impure droplets because of the correspondingly more sluggish kinetics.

### 4. Theoretical values of solid-liquid energies

In view of the paucity until recently of directly measured values of interfacial energy, some attention has been paid to deriving calculated values from theoretical models of the solid-liquid interface. Because of the complexity of cases involving either impure systems, or rapidly moving interfaces, such treatments have almost all been restricted to pure materials at equilibrium. Even in the latter instance, however, the structure of a real solid-liquid interface is likely to be far more complex than that of a model interface suited to quantitative treatment. There is the added problem that a model cannot easily take into account the effect of the adsorbed monolayers that are probably always present at solid-liquid interfaces. We should not, therefore, rely on calculated energy values; rather, they should be compared with reliable experimental figures in order to tell us something about the validity of the theoretical models.

A series of detailed comparisons between experimental and theoretical values of  $\gamma_{SL}$  merits an extended study and is not suited to the scope of this paper. However, it is profitable to discuss the results of a representative group of theoretical treatments in relation to those materials for which  $\gamma_{SL}$  has been measured directly (see Table I). Skapski [83] has developed what appears to be a reasonable [81] model, based on pairwise bonding, for calculating solid-vapour energies. Unfortunately, in order to calculate  $\gamma_{SL}$  from the surface energies, it has to be assumed that

$\gamma_{SV} = \gamma_{SL} + \gamma_{LV}$ . There is no real physical justification for this result [12]; in fact there is experimental evidence that in some systems  $\gamma_{SV} < \gamma_{SL} + \gamma_{LV}$  [12, 46, 84, 85], whereas in others  $\gamma_{SV}$  may well be greater than  $\gamma_{SL} + \gamma_{LV}$  [81]. Thus Skapski's figures for lead and gold cannot be compared with those in Table I.

A different approach has been adopted by Kotzé and Kuhlmann-Wilsdorf [86] who calculated the energies of high-angle grain boundaries for a range of materials, and, with no physical justification, assumed  $\gamma_{SL}$  to be half the grain-boundary energy. For the materials common to this treatment and to Table I, this assumption appears to have been verified *experimentally* for ice-water [23, 24] and possibly bismuth [47]. The calculated values of 39 and 68  $\text{mJ m}^{-2}$  for these materials agree surprisingly well with the directly measured values of  $44 \pm 10$  and  $74 \pm 3 \text{ mJ m}^{-2}$  respectively.

A third approach has been adopted by Ewing [87, 88] who assumed that the solid remains undistorted up to the interface, but that the positioning of atoms in the liquid normal to the interface is described by the radial distribution function of the given materials. The entropy contribution to  $\gamma_{SL}$ ,  $S$ , was calculated from the shape of the distribution function. The contribution of the crystal surface to  $\gamma_{SL}$  was calculated using the relation  $\gamma_{SL}(\text{crystal}) = nL(\text{molar})/4N$ , where  $n$  is the number density of atoms in the surface (assumed planar) and  $N$  is Avogadro's number.  $\gamma_{SL}$  was taken to be the sum of  $\gamma_{SL}(\text{crystal})$  and  $T_m |S|$ . Using published experimental data on the radial distribution function  $\gamma_{SL}$  was calculated for six metals. Considering the materials listed in Table I, values were calculated for lead and gold of 53 and 148  $\text{mJ m}^{-2}$  respectively. These values are in rather poor agreement with experiment, possibly reflecting the various sources of error mentioned by Ewing. Nevertheless the model is a welcome attempt in recognizing and attempting to quantify the probably diffuse nature of the interface.

Finally, quantitative progress appears to have been made [89] in setting up a model where the crystal surface has a hill-and-dale formation, but where the surface is distinct or non-diffuse (i.e. an atom can be assigned definitely either to the liquid or to the solid phase). It would in general appear necessary to marry the two latter approaches in order to formulate a realistic

model of solid-liquid interfaces.

## 5. Empirical formulae for solid-liquid energies

In order to be able to predict values of  $\gamma_{SL}$  for given applications it would be most useful to have recourse to empirical formulae. A useful result may be adapted from the one given by Turnbull [90] such that

$$\gamma_{SL}(\text{experimental}) = KL(\text{molar})n/N, \quad (5)$$

where  $K$  is an empirical constant. The values of  $K$  obtained from the direct values of  $\gamma_{SL}$  at present available (Table I) are plotted in Fig. 10 against  $L(\text{molar})/T_m R$ , where  $R$  is the gas constant. It is very encouraging that for nearly all materials having a comparatively low value of  $L(\text{molar})/T_m R$  (and possibly having roughly spherical atoms or molecules)  $K$  is practically constant. However, for substances having more asymmetrical molecules, the appropriate value of  $K$  increases noticeably. The increased scatter observed in the latter region of the graph may well reflect anisotropies of interfacial energy or gross differences in crystal structure. Undoubtedly correlations of the present type overlook some important pieces of physics; but they would seem capable of predicting interfacial energies quite accurately for many materials.

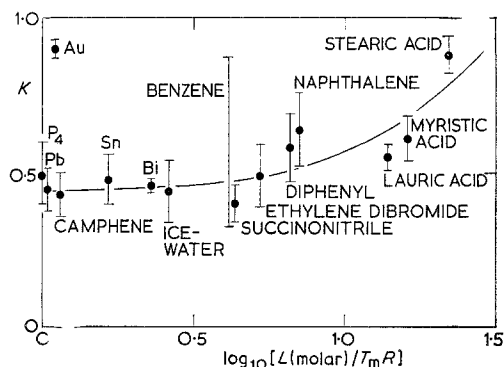


Figure 10 Values of  $K$  (calculated from directly measured energies according to Equation 5) plotted against  $L(\text{molar})/T_m R$ .

## 6. Conclusion

In summary, the experimental work of the last few years appears to have established a sound body of information on solid-liquid energies. It is especially pleasing that, as illustrated by the

studies on ice-water, four distinct methods of measuring  $\gamma_{SL}$  directly are capable of producing extremely consistent results. In particular the work indicates the inherent reliability of the new groove-shape technique, which is most encouraging in view of the flexibility and relative convenience of the method. By exerting, for example, better control over the thermal configuration of the experimental system it should be relatively easy to improve significantly the accuracy obtainable with the technique; and the results of applying the method to alloyed systems are likely to be very rewarding.

### Acknowledgements

The author wishes to thank Professor R. W. K. Honeycombe for the provision of research facilities. He is also indebted to the Science Research Council for their support and to the Master and Fellows of Christ's College, Cambridge for help in the form of a Fellowship.

### References

1. M. J. STOWELL, *Phil. Mag.* **22** (1970) 1.
2. D. TURNBULL, *J. Chem. Phys.* **18** (1950) 198.
3. J. W. CAHN, W. B. HILLIG and G. W. SEARS, *Acta Metallurgica* **12** (1964) 1421.
4. S. C. HARDY and S. R. CORIELL, *J. Crystal Growth* **5** (1969) 329.
5. G. R. KOTLER and L. A. TARSHIS, *ibid* **3, 4** (1968) 603.
6. G. F. BOLLING and W. A. TILLER, *J. Appl. Phys.* **31** (1960) 1345.
7. D. R. H. JONES, *J. Crystal Growth* **16** (1972) 187.
8. W. A. MILLER and G. A. CHADWICK, *Acta Metallurgica* **15** (1967) 607.
9. R. C. TOLMAN, *J. Chem. Phys.* **17** (1949) 333.
10. J. G. KIRKWOOD and F. P. BUFF, *ibid* **17** (1949) 338.
11. F. P. BUFF and J. G. KIRKWOOD, *ibid* **18** (1950) 991.
12. C. J. COOMBES, Ph.D. Thesis, London University (1969).
13. C. R. M. WRONSKI, *Brit. J. Appl. Phys.* **18** (1967) 1731.
14. J. R. SAMBLES, *Proc. R. Soc. A* **324** (1971) 339.
15. C. J. COOMBES, *J. Phys. F.* **2** (1972) 441.
16. W. DROST-HANSEN, private communication.
17. F. MEISSNER, *Z. Anorg. u. Allgem. Chem.* **110** (1920) 169.
18. R. C. SILL and A. S. SKAPSKI, *J. Chem. Phys.* **24** (1956) 644.
19. A. S. SKAPSKI, R. BILLUPS and A. ROONEY, *ibid* **26** (1957) 1350.
20. A. S. SKAPSKI, R. BILLUPS and D. CASAVANT, *ibid* **31** (1959) 1431.
21. E. S. MIKSCH, *Rev. Sci. Instrum.* **36** (1965) 797.
22. D. R. H. JONES, Ph.D. Thesis, Cambridge University (1970).
23. W. M. KETCHAM and P. V. HOBBS, *Phil. Mag.* **19** (1969) 1161.
24. M. E. R. WALFORD, unpublished work, referred to by J. F. NYE and S. MAE, *J. Glaciol.* **11** (1972) 81.
25. G. KANIG, *Kolloid Z.* **173** (1960) 97.
26. P. KUBELKA and R. PROKSCHA, *ibid* **109** (1944) 79.
27. B. R. PURI, L. R. SHARMA and M. L. LAKHANPAL, *J. Chem. Phys.* **58** (1954) 289.
28. B. R. PURI, D. D. SINGH and Y. P. MYER, *Trans. Faraday Soc.* **53** (1957) 530.
29. J. L. SHERESHEFVSKY, *J. Amer. Chem. Soc.* **50** (1928) 2966.
30. M. FOLMAN and J. L. SHERESHEFVSKY, *J. Phys. Chem.* **59** (1955) 607.
31. W. J. O'BRIEN, *Surf. Sci.* **19** (1970) 387.
32. A. R. UBBELOHDE, "Melting and Crystal Structure" (Clarendon Press, Oxford, 1965) p. 29.
33. G. E. NASH and M. E. GLICKSMAN, *Phil. Mag.* **24** (1971) 577.
34. D. R. H. JONES and G. A. CHADWICK, *ibid* **22** (1970) 291.
35. *Idem*, *J. Crystal Growth* **11** (1971) 260.
36. D. R. H. JONES, *Phil. Mag.* **27** (1973) 569.
37. *Idem*, *Rev. Sci. Instrum.* **41** (1970) 1509.
38. L. R. MORRIS, unpublished work [mentioned in 33].
39. D. P. WOODRUFF and A. J. FORTY, *Phil. Mag.* **15** (1967) 935.
40. T. R. ANTHONY and H. E. CLINE, *J. Appl. Phys.* **43** (1972) 2473.
41. E. W. J. MILLER and J. BEECH, *Metallography* **5** (1972) 298.
42. H. E. CLINE and T. R. ANTHONY, *Acta Metallurgica* **19** (1971) 491.
43. D. R. H. JONES and G. A. CHADWICK, *Phil. Mag.* **24** (1971) 1327.
44. D. R. H. JONES, *J. Crystal Growth*, in press.
45. S. SUZUKI and D. KUROIWA, *J. Glaciol.* **11** (1972) 265.
46. C. A. KNIGHT, *Phil. Mag.* **23** (1971) 153.
47. M. E. GLICKSMAN and C. L. VOLD, *Acta Metallurgica* **17** (1969) 1.
48. *Idem*, *Scripta Met.* **5** (1971) 493.
49. R. A. MASAMURA, M. E. GLICKSMAN and C. L. VOLD, *ibid* **6** (1972) 943.
50. D. TURNBULL and J. C. FISHER, *J. Chem. Phys.* **17** (1949) 71.
51. J. H. HOLLOMAN and D. TURNBULL, *Prog. Met. Phys.* **4** (1953) 333.
52. K. A. JACKSON, *Ind. Eng. Chem.* **57** (1965) 29.
53. D. TURNBULL, *J. Chem. Phys.* **20** (1952) 411.
54. I. E. KUHN and B. J. MASON, *Proc. R. Soc. A* **302** (1968) 437.
55. G. R. WOOD and A. G. WALTON, *J. Appl. Phys.* **41** (1970) 3027.
56. G. L. F. POWELL, *J. Aust. Inst. Metals* **10** (1965) 223.
57. D. W. GOMMERSALL, S. Y. SHIRASHI and R. G. WARD, *ibid* **10** (1965) 220.



58. B. VONNEGUT, *J. Colloid. Sci.* **3** (1948) 563.
59. D. TURNBULL and R. E. CECH, *J. Appl. Phys.* **21** (1950) 804.
60. D. R. H. JONES and G. A. CHADWICK, *Phil. Mag.* **24** (1971) 995.
61. J. E. HILLIARD and J. W. CAHN, *Acta Metallurgica* **6** (1958) 772.
62. W. JACOBI, *Z. Naturforsch A* **10** (1955) 322.
63. B. J. MASON, "The Physics of Clouds" (University Press, Oxford, 1957) p. 128.
64. L. DUFOUR and R. DEFAY, "Thermodynamics of Clouds" (Academic Press, New York, 1963) p. 231.
65. G. R. WOOD and A. G. WALTON, unpublished work.
66. S. C. HARDY, S. R. CORIELL and R. F. SEKERKA, *J. Crystal Growth* **11** (1971) 53.
67. S. C. HARDY and S. R. CORIELL, *ibid* **7** (1970) 147.
68. *Idem*, *ibid* **3, 4** (1968) 569.
69. D. P. WOODRUFF, private communication.
70. D. E. TEMKIN, *Dokl. Akad. Nauk. SSSR* **132** (1960) 1307.
71. G. R. KOTLER and L. A. TARSHIS, Publication Preprint, Ford Scientific Laboratory, Dearborn, Michigan, USA (1968).
72. M. E. GLICKSMAN and R. J. SCHAEFER, *J. Crystal Growth* **1** (1968) 297.
73. R. TRIVEDI, *Acta Metallurgica* **18** (1970) 287.
74. G. R. KOTLER, private communication.
75. R. FERNANDEZ and A. J. BARDUHN, *Desalination* **3** (1967) 330.
76. H. E. CLINE and T. R. ANTHONY, *Acta Metallurgica* **19** (1971) 175.
77. U. M. FRANKLIN and W. A. MILLER, *Canad. Met. Q.* **8** (1969) 145.
78. W. A. MILLER and G. A. CHADWICK, *Proc. R. Soc. A* **312** (1969) 257.
79. *Idem*, in "The Solidification of Metals" (The Iron and Steel Institute, London, 1968) p. 49.
80. H. SANG, W. A. MILLER and G. A. CHADWICK, to be published.
81. G. A. CHADWICK, in "Interfaces" (edited by R. C. Gifkins) (Butterworths, London, 1969) p. 101.
82. J. BASTERFIELD, W. A. MILLER and G. C. WEATHERLY, *Canad. Met. Q.* **8** (1969) 131.
83. A. S. SKAPSKI, *Acta Metallurgica* **4** (1956) 576.
84. F. K. GORSKII and A. S. MIKULICH, in "Crystallization Processes" (edited by N. N. Sirota, F. K. Gorskii and V. M. Varikash) English Translation (Consultants Bureau, New York, 1964) p. 3.
85. M. BLACKMAN, S. J. PEPPIATT and J. R. SAMBLES, *Nature Lond.* **239** (1972) 61.
86. I. A. KOTZÉ and D. KUHLMANN-WILSDORF, *Appl. Phys. Letters* **9** (1966) 96.
87. R. H. EWING, *Phil. Mag.* **25** (1972) 779.
88. *Idem*, *J. Crystal Growth* **11** (1971) 221.
89. D. E. TEMKIN, in "Crystallization Processes" (edited by N. N. Sirota, F. K. Gorskii, and V. M. Varikash) English Translation (Consultants Bureau, New York, 1964) p. 15.
90. D. TURNBULL, in "Liquids: Structure, Properties, Solid Interactions" (edited by T. J. Hughel) (Elsevier, Amsterdam, London and New York, 1965) p.6.
91. D. G. THOMAS and L. A. K. STAVELEY, *J. Chem. Soc.* **1952** (1952) 4569.

Received 8 February and accepted 4 July 1973.